Available online at www.sciencedirect.com
SCIENCE DIRECT
Thermochimica Acta 444 (2006) 173–178
thermochimica acta
www.elsevier.com/locate/tca

Structure and crystallization kinetics of Bi_2O_3–B_2O_3 glasses

Yin Cheng, Hanning Xiao *, Wenming Guo, Weiming Guo

College of Materials Science and Engineering, Hunan University, Changsha, Hunan 410082, China

Received 26 December 2005; received in revised form 7 March 2006; accepted 13 March 2006
Available online 22 March 2006

Abstract

The experimental IR (infrared spectra) and differential scanning calorimetry (DSC) curves of Bi_2O_3–B_2O_3 glasses, containing 30–60 mol% Bi_2O_3, have been investigated in the article. The composition dependence of IR absorption suggests that addition of Bi_2O_3 results in a change in the short-range order structure of the borate matrix. The increase of Bi_2O_3 content causes a progressive conversion of [BO_3] to [BO_4] units. Bi_2O_3, in the form of [BiO_6] octahedral units, plays the role of glass former. The crystallization kinetics of Bi_2O_3–B_2O_3 glasses were described by thermal stability indexes (k_{gl}, ΔT), activation energy (E) for crystallization and numerical factors(n, m) depending on the nucleation process and growth morphology, which were calculated by Šatava method and the modified Ozawa–Chen method. When $Bi_2O_3 \leq 45$ mol%, the increase of Bi_2O_3 tends to improve the thermal stabilities of the glasses. In this case, k_{gl} may be more suitable for estimating the glass thermal stability in above composition range than ΔT. A further increase of Bi_2O_3 content will increase the crystallization trends of investigated glasses. Two possible kinds of growth mechanisms were involved in Bi_2O_3–B_2O_3 glasses: one-dimensional growth and two-dimensional growth. Moreover, structures of crystallized glasses were observed by X-ray diffraction (XRD). $BiBO_3$ crystal with special non-linear optical properties can be obtained when $Bi_2O_3 \geq 50$ mol%.

Keywords: Crystallization kinetics; Glass structure; DSC

1. Introduction

Having a high potential for extensive industrial application to laser host, tunable waveguide, tunable fiber grating, and so on, crystallized glasses consisting of non-linear optical crystals have been given many attentions recently. For instance, transparent crystallized glasses consisting of $LaBGeO_5$, $SrBi_2Ta_2O_9$ and $Ba_2TiGe_2O_8$, which are noble optical non-linear and ferroelectric crystals, have been fabricated [1–3]. Very recently new non-linear optical crystalline phases BiB_3O_6 was formed showing up larger non-linear optical coefficients than those of other non-linear optical materials being used [4]. On the other hand, Ihara et al. [5] suggested that the metastable $BiBO_3$ crystal be a new candidate for non-linear optical materials. Since these two crystals are all bismuth borate crystals, a further study on optical properties of Bi_2O_3–B_2O_3 glasses has been of great significance [6,7]. Isabella-Ioana Opera et al. have investigated the optical properties of Bi_2O_3–B_2O_3 glasses [6] and their study indicates that the optical properties of bismuth borate glasses are mainly influenced by the bismuth oxide group, at least in the short wavelength region. Studies on rare-earth ions-doped Bi_2O_3–B_2O_3 glasses [8–10] show that the structure of $BiBO_3$ crystal is stabilized by substitution of rare-earth ions for Bi^{3+}, presenting excellent non-linear optical properties.

It is well known that structure has a crucial influence on properties of materials. The building of relationship between structure and crystallization of Bi_2O_3–B_2O_3 glasses should be of great importance for better understanding the special optical properties of this material. Whereas there are only few reports on structure study of rare-earth and transition metal ions-doped Bi_2O_3–B_2O_3 glasses [11,12]. No systemic report was found on binary Bi_2O_3–B_2O_3 glasses to our knowledge. This paper aims to demonstrate the structure and crystallization kinetics of Bi_2O_3–B_2O_3 glasses, with a wide composition range of 30 mol% $\leq Bi_2O_3 \leq$ 60 mol%.

2. Theoretical basis

DSC is very effective for determining the kinetic parameters of glass crystallization under non-isothermal conditions

* Corresponding author. Tel.: +86 731 8822269; fax: +86 713 2617678.
E-mail address: zjbcy@126.com (H. Xiao).

0040-6031/$ – see front matter © 2006 Elsevier B.V. All rights reserved.
doi:10.1016/j.tca.2006.03.016

Table 1
The values of n and m for various crystallization mechanisms [19]

Mechanism	n	m
Bulk crystallization		
Three-dimensional growth	4	3
Two-dimensional growth	3	2
One-dimensional growth	2	1
Surface crystallization	1	1

[13–15]. The modified Johnson–Mehl–Avrami (JMA) equation is often used to describe the behavior of non-isothermal glass crystallization [16]:

$$\ln[-\ln(1-\alpha)] = -n\ln b - 1.052\frac{mE_G}{RT} + \text{const.} \quad (1)$$

where α is the volume fraction of crystals precipitated in glass which can be estimated by the area of crystallization exothermal peak [17], n and m factors depending on the nucleation process and growth morphology, R the universal gas constant, and E_G is the activation energies for crystal growth. The effective activation energy of the crystallization process E can be defined by $E = (m/n)E_G$. When nuclei are formed during the heating at a constant rate b are dominant, n is equal to $(m + 1)$, whereas when nuclei are formed in the previous heat treatment before thermal analysis run are dominant, n is equal to m [18]. The values of n and m are listed in Table 1.

From Eq. (1), E_G and n can be evaluated simply by Šatava method [18]:

$$\left.\frac{\mathrm{d}\ln[-\ln(1-\alpha)]}{\mathrm{d}(1/T)}\right|_b = -1.052\frac{mE_G}{R}c \quad (2)$$

and the modified Ozawa–Chen method [19,20]:

$$\left.\frac{\mathrm{d}(\ln b)}{\mathrm{d}(1/T)}\right|_\alpha = -1.052\frac{m}{n}\frac{E_G}{R} \quad (3)$$

DSC also helps to determine the glass characteristic temperatures, such as glass transition temperature T_g, onset crystallization temperature T_x, and liquidus temperature T_l. These thermal parameters are important for a qualitative estimation of the thermal stability and forming ability of glasses. For example, to estimate the glass stability one usually uses the thermal stability index, defined by $\Delta T = T_x - T_g$ [21], while the glass forming ability (k_{gl}), introduced by Hruby Czech [22], is expressed as the following:

$$k_{gl} = \frac{T_x - T_g}{T_l - T_x} \quad (4)$$

The bigger difference $\Delta T = T_x - T_g$ and the smaller temperature interval $T_l - T_x$ indicate the more stable for glasses and lower tendency of crystallization.

3. Experiments

The Bi_2O_3–B_2O_3 glasses with Bi_2O_3 content ranging Bi_2O_3 from 30 to 60 mol%, were prepared by conventional melting–quenching method with analytic reagent (AR) grade Bi_2O_3 and B_2O_3 as raw materials. After homogenization, the batches were melted in the temperature range of 700–1000 °C and the resulting liquid quenched in graphite mould, then crystallized at crystallization peak temperatures for 1 h. The compositions of glasses are shown in Table 2. Transparent and homogeneous glasses were obtained.

Table 2
The compositions of Bi_2O_3–B_2O_3 glasses

No.	BiB-1	BiB-2	BiB-3	BiB-4	BiB-5	BiB-6	BiB-7
Content of Bi_2O_3 (mol%)	0.3	0.35	0.4	0.45	0.5	0.55	0.6

The infrared spectra of the glasses were recorded at room temperature, immediately after glass preparation, using KBr disc technique. A Bruker IFS66V spectrometer was used to obtain the spectra in the wave number range between 400 and 2000 cm^{-1} with a resolution of 2 cm^{-1}. DSC measurements were performed by Netzsch STA449C calorimeter at different heating rates (5, 10, and 20 °C/min). The structure of crystallized phases in the glasses after crystallization was analyzed by XRD using Cu K_α radiation in a Rigaku D/Max 2550VB$^+$ 18 kW equipment with a rotating anode.

4. Results and discussion

4.1. Structure analysis of Bi_2O_3–B_2O_3 glasses

The infrared absorption spectra of Bi_2O_3–B_2O_3 glasses are shown in Fig. 1. Table 3 and Table 4 summarize the major absorption bands observed in the investigated glasses and their vibration types, respectively.

In the infrared spectra of Bi_2O_3–B_2O_3 glasses (Fig. 1), as Bi_2O_3 content increases, the band at 521 cm^{-1}, contributing

Table 3
Observed IR absorption bands in Bi_2O_3–B_2O_3 glass system

No.	IR absorption bands (cm^{-1})			
BiB-1	1333	943	681	521
BiB-2	1325	943	681	494
BiB-3	1309	924	690	503
BiB-4	1294	918	694	507
BiB-5	1279	906	687	499
BiB-6	1250	901	698	457
BiB-7	1242	899	698	438

Table 4
Vibration types of different IR wave numbers

Range of wave numbers (cm^{-1})	Vibration types
420–520	Bi—O—Bi vibration of [BiO_6] octahedral units [23,24]
680–720	Bending vibration of B—O—B in [BO_3] triangles [25,26]
900–950	Stretching vibration of [BO_4] units [27]
1200–1300	Stretching vibration of B—O—B in [BO_3] triangles [25,26]

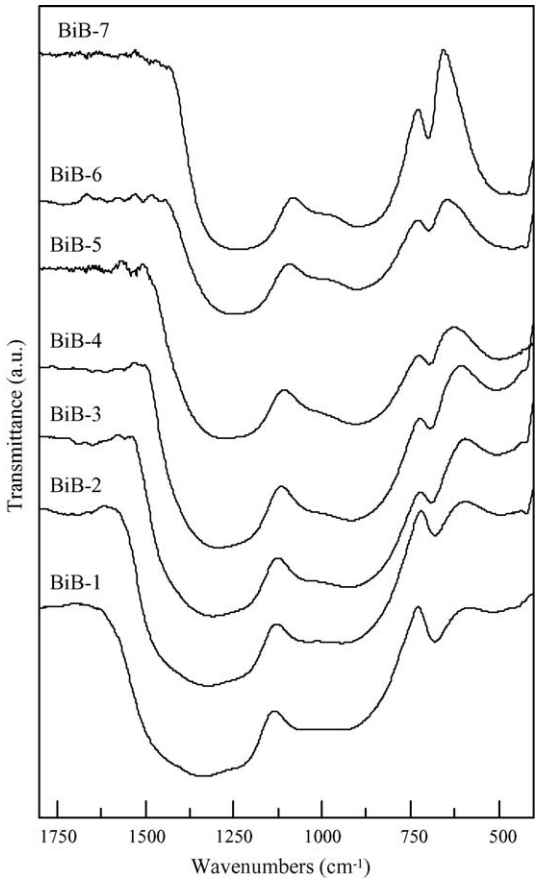

Fig. 1. Infrared absorption spectra of Bi_2O_3–B_2O_3 glasses.

to the Bi–O–Bi vibration of distorted [BiO_6] octahedral units [23,24], increases in intensity and shifts to lower wave numbers. Since the [BiO_3] polyhedra vibration band at 840 cm^{-1} [28] does not appear in the IR absorption, it can be concluded that only [BiO_6] octahedral units build up the bismuthate structure of investigated glasses. In contrast, A larger shift was observed at the band from 681 to 698 cm^{-1}, which belongs to the bending vibration of B–O–B in [BO_3] units [25,26]. This shift may be introduced by the electrostatic field of the strongly polarizing Bi^{2+} ions. The raising Bi_2O_3 content results in the increase of the electron cloud density around oxygen of [BO_3] unit, thus leads to increase the roll-torque of B–O–B band and consequently contributes to the bending vibration of B–O–B band shifts to a higher wave number.

Table 5
Thermal characteristics of Bi_2O_3–B_2O_3 glasses

No.	T_g (°C)	T_x (°C)	T_l (°C)	ΔT (°C)	k_{gl}
BiB-1	461.2		710.5		
BiB-2	446.2	587.6	724.7	141.4	1.03
BiB-3	409.6	536.4	658.2	126.8	1.04
BiB-4	384.9	494.4	590.8	109.5	1.14
BiB-5	380.0	471.5	607.0	91.5	0.68
BiB-6	379.5	447.8	584.4	68.3	0.50
BiB-7	349.9	417.5	577.0	67.6	0.42

The infrared spectral range of 900–950 cm^{-1} is typical for the stretching vibration of [BO_4] units [27]. The existence of [BO_4] units indicates that the addition of Bi_2O_3 to B_2O_3 causes a progressive conversion of [BO_3] units to [BO_4] units. Bands between 1200 and 1300 cm^{-1} are assigned to the stretching vibration of [BO_3] units [25,26]. As the Bi_2O_3 content increased, both bands decrease in intensity and shift to lower wave numbers. This may be explained by accepting the assumption that new bridging bond of Bi–O–B is formed by the inducement of strongly polarizing Bi^{3+} ions. Since the stretching force constant of Bi–O bonding is substantially lower than that of the B–O, the stretching frequency of Bi–O–B might trend to be lower.

4.2. Crystallization kinetics of Bi_2O_3–B_2O_3 glasses

The DSC curves from the different stoichiometries were indicated in Fig. 2. Values of characteristic temperatures summarized in Table 5 were extracted using the Proteus software installed in the DSC instrument. T_g was the inflection temperature of glass transition, T_x was the onset temperature of exothermic peak, and T_l was the peak point of endothermic peak for melting. For BiB-1 sample, no exothermic peak observed indicates that the glass have little trend to crystallize before

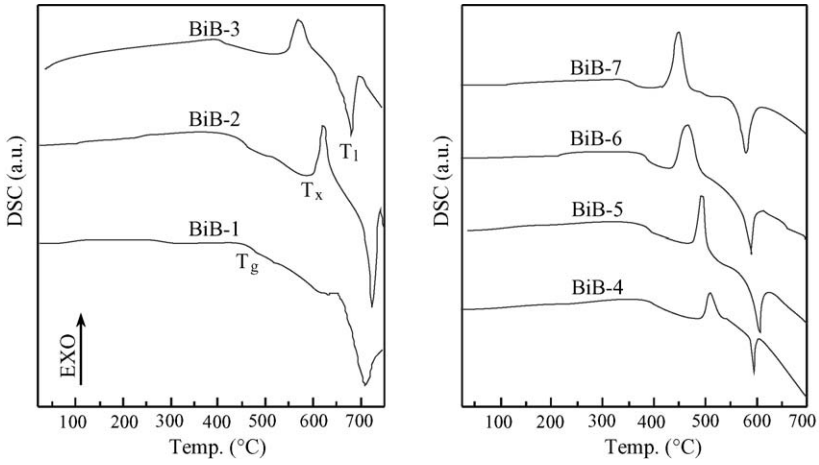

Fig. 2. DSC curves for Bi_2O_3–B_2O_3 glasses.

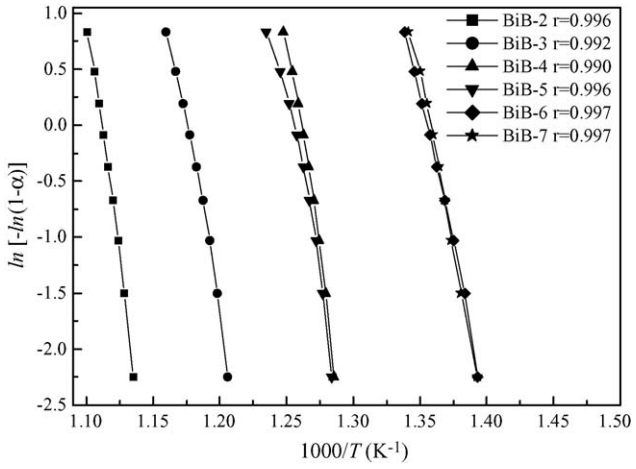

Fig. 3. Determination of mE_G according to the Šatava method by plotting $\ln[-\ln(1-\alpha)]$ vs. $1/T$ at heating rate $b = 10\,^{\circ}$C/min. r is the correlative coefficient of linear fitting.

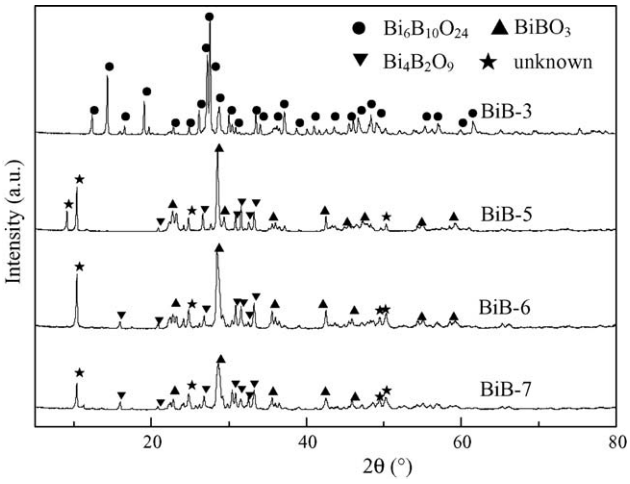

Fig. 5. XRD patterns of crystallized glasses heat-treated at around crystallization temperatures for 1 h in Bi_2O_3–B_2O_3 glasses.

Table 6
Kinetic parameters of crystallization of Bi_2O_3–B_2O_3 glass system calculated by different methods

No.	n	m	mE_G (kJ/mol)	E_G (kJ/mol)	$E = (m/n)E_G$ (kJ/mol)
BiB-2	3.27	2	699.39	349.70	214.05
BiB-3	2.32	1	511.25	511.25	220.03
BiB-4	2.02	1	632.58	632.58	312.62
BiB-5	1.91	1	485.14	485.14	254.62
BiB-6	1.72	1	430.95	435.28	250.35
BiB-7	1.99	1	486.71	427.52	244.12

melting. Therefore, calculations of crystallization kinetics were carried out on other samples except BiB-1. Šatava method (Eq. (2)) was used to evaluate the values of mE_G and a constant heating rates at 10 °C/min was assumed, as shown in Fig. 3. The volume fraction of crystals α of each sample in Fig. 3 was the same and lied in the range of 0.1–0.9. The correlation coefficients r of the plots are all greater than 0.99 indicating good linear relationships. The values of $E = (m/n)E_G$ were calculated by Ozawa–Chen method (Eq. (3)) at the range of $\alpha = 0.05$–0.95. The mean value at different values of α was chosen as the effective energy E for each sample, which was listed in Table 6. Fig. 4 demonstrates the dependence of E on the extent of α. With the increase of α, E decreases especially in sample BiB-5, -6 and -7. This effect is also supported by the crystallization theory of Vyazovkin and Dranca [29]. By comparing the activation energy at the same extent of α, e.g. $\alpha = 0.4$, their values are 208 kJ/mol (BiB-2), 217 kJ/mol (BiB-3), 319 kJ/mol (BiB-4), 253 kJ/mol (BiB-5), 226 kJ/mol (BiB-6), and 174 kJ/mol (BiB-7), respectively. This trend suggests that the dependence of E on the extent of α has a transition at the sample of BiB-4. The values of n, m and E_G were estimated by combined the results above, assuming that nucleation rate is constant ($n = m + 1$). All values of the kinetic parameters of crystallization above were summarized in Table 6.

From the results of the kinetic criteria ΔT, k_{gl} (Table 5) and the activation energies (Table 6), it is possible to make conclusions for the competitive role of Bi_2O_3 and B_2O_3 as a conditional network former. Table 5 indicates that the glass transition and crystallization temperatures decrease with the increase of Bi_2O_3 content. The change of glass thermal stabilities can be divided into the following two regions:

(1) For $35 \le Bi_2O_3 \le 45$ mol%, the values of ΔT are over 100 °C and decrease at higher Bi_2O_3 content. Whereas an increasing trend is observed in another parameter of glass thermal stability k_{gl}. The change of the activation energy for crystallization, E (see Table 6) is consistent with that of k_{gl}, which indicates that higher glass thermal stability against crystallization can be obtained as Bi_2O_3 content increased.

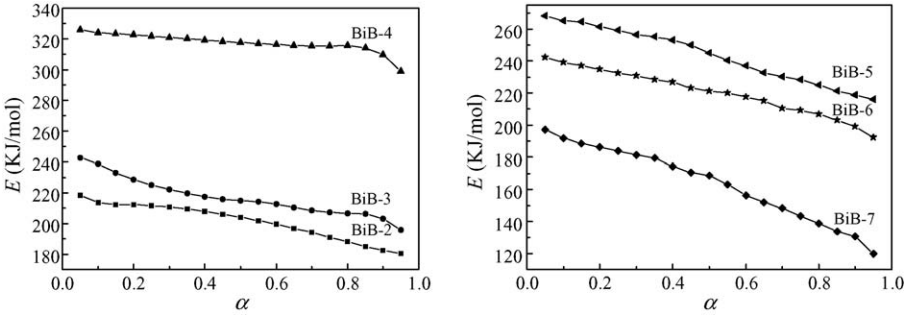

Fig. 4. $E = (m/n)E_G$ as a function of the extent of crystallization α obtained by Ozawa–Chen method.

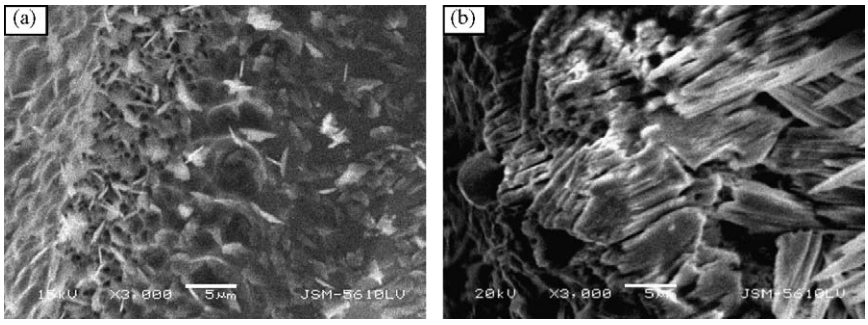

Fig. 6. SEM graphs of crystallized samples (a) BiB-2; (b) BiB-4.

Therefore, it can be suggested that k_{gl}, compared with ΔT, may be more compatible for estimating the glass thermal stability in the glasses.

(2) As Bi_2O_3 content is larger than 50 mol%, the values of ΔT and k_{gl} are lower, which are below 100 °C and 1.0, respectively, suggesting that the glass stability in this region is much lower than that in $35 \leq Bi_2O_3 \leq 45$ mol%. The decrease of ΔT, k_{gl} and E with the increase of Bi_2O_3 content shows that Bi_2O_3 increases the trend of crystallization, which may be important for Bi_2O_3–B_2O_3 glasses as promising materials for non-optical applications.

The different values of n and m indicate the different crystallization mechanisms. According to the results in Table 1 and Table 6, BiB-2 corresponds to two-dimensional growth, while the crystal growth of other samples are all controlled by one-dimensional growth mechanism.

4.3. Crystals investigation

Fig. 5 shows the XRD patterns of crystallized glasses heat-treated at the vicinity of crystallization temperatures for 1 h. The crystals of $Bi_6B_{10}O_{24}$, $Bi_4B_2O_9$ and $BiBO_3$ were observed in the glasses. There are several peaks that cannot be clarified by JCPDS cards. $BiBO_3$ crystal, which is a promising non-linear optical crystal [5], is observed in BiB-5 and -7 samples, which means that the $BiBO_3$ crystal can only formed with Bi_2O_3 content over 45 mol%. Therefore, the crystallization of Bi_2O_3–B_2O_3 glasses may be one of the effective methods for realizing the special non-linear optical properties, attributed to the formation of $BiBO_3$ crystal.

The morphology of the crystals in the crystallized glasses was investigated by SEM. Two types of crystals were observed: BiB-2 is lamellar, while other samples are needle-like. As a representative, the SEM graphs of BiB-2 and -4 samples were shown in Fig. 6. Therefore, the results of SEM are consistent with that of crystallization kinetics.

5. Conclusions

The addition of Bi_2O_3 results in variation of the structure and crystallization kinetics of Bi_2O_3–B_2O_3 glasses ($30 \leq Bi_2O_3 \leq 60$ mol%). The basis network structure of Bi_2O_3–B_2O_3 glasses consists of chains with $[BO_3]$, $[BO_4]$ and $[BiO_6]$ units. For $35 \leq Bi_2O_3 \leq 45$ mol%, the increase of Bi_2O_3 improves the glass stability against crystallization. The crystal growth can be controlled by two mechanisms: one- and two-dimension growth. Further increase of Bi_2O_3 content brings enlarged crystallization trends of investigated glasses. Non-linear optical crystal, $BiBO_3$, was obtained in the range of $50 \leq Bi_2O_3 \leq 60$ mol%. In this case, the crystallization of the glasses corresponds to one-dimensional growth mechanism.

Acknowledgments

The work was supported under the National Natural Science Foundation of China: No. 50174024. We thank Ms. Chui Hui and Ms. Li De-Yi for the IR and XRD measurements of the glasses.

References

[1] Y. Takahashi, Y. Benino, T. Fujiwara, T. Komatsu, J. Appl. Phys. 89 (2001) 5282–5287.
[2] G.S. Murugan, K.B.R. Varma, Y. Takahashi, T. Komatsu, Appl. Phys. Lett. 78 (2001) 4019–4021.
[3] Y. Takahashi, Y. Benino, T. Fujiwara, T. Komatsu, J. Appl. Phys. 95 (2004) 3503–3508.
[4] H. Hellwig, J. Liebertz, L. Bohatý, J. Appl. Phys. 88 (2000) 240–244.
[5] R. Ihara, T. Honma, Y. Fujiwara, T. Komatsu, Opt. Mater. 27 (2004) 403–408.
[6] Isabella-Ioana Opera, Hartmut Hesse, Klaus Betzler, Opt. Mater. 26 (2004) 235–237.
[7] R. Ihara, Y. Benino, T. Fujiwara, T. Komatsu, Adv. Mater. 6 (2005) 138–142.
[8] M.B. Saisudha, J. Ramakrishna, Opt. Mater. 18 (2002) 403–417.
[9] T. Honma, Y. Benino, T. Fujiwara, R. Sato, T. Komatsu, Opt. Mater. 20 (2002) 27–33.
[10] Y.J. Chen, Y.D. Huang, M.L. Huang, R.P. Chen, Z.D. Luo, Opt. Mater. 25 (2004) 271–278.
[11] L. Baia, R. Stefan, W. Kiefer, J. Popp, S. Simon, J. Non-Cryst. Solids 303 (2002) 379–386.
[12] B. Karthikeyan, S. Mohan, Physica B 334 (2003) 298–302.
[13] C. Dayanand, M. Salagram, Ceram. Int. 30 (2004) 1731–1735.
[14] R. Iordanova, E. Lefterova, I. Uzunov, Y. Dimitriev, D. Klissurski, J. Therm. Anal. Calorim. 70 (2002) 393–404.
[15] K. Yukimitu, R.C. Oliveira, E.B. Araújo, J.C.S. Moraes, L.H. Avanci, Thermochim. Acta 426 (2005) 157–161.
[16] H. Yinnon, D.R. Uhlmann, J. Non-Cryst. Solids 54 (1983) 253–275.
[17] C.S. Ray, W.H. Huang, D.E. Day, J. Am. Ceram. Soc. 74 (1991) 60–66.
[18] K. Matusita, S. Sakka, Phys. Chem. Glasses 20 (4) (1979) 81–84.
[19] T. Ozawa, Bull. Chem. Soc. Jpn. 38 (1965) 1881–1886.

[20] H.S. Chen, J. Non-Cryst. Solids 27 (1978) 257–263.
[21] S. Mahadevan, A. Giridhar, A.K. Singh, J. Non-Cryst. Solids 88 (1986) 11–34.
[22] A. Hruby Czech, Physica B 22 (1972) 1187–1193.
[23] Y. Dimitriev, M. Mihailova, Proceedings of the 16th International Congress on Glass, vol. 3, Madrid, 1992, p. 293.
[24] M.E. Lines, A.E. Miller, K. Nassau, K.B. Lyons, J. Non-Cryst. Solids 89 (1987) 163–180.
[25] E.I. Kamitsos, A.P. Patsis, M.A. Karakassides, G.D. Chryssikos, J. Non-Cryst. Solids 126 (1990) 52–67.
[26] A.K. Hassan, L. BÖrjesson, L.M. Torell, J. Non-Cryst. Solids 172/174 (1994) 154–160.
[27] G. El-Damrawi, K. El-Egili, Physica B 299 (2001) 180–186.
[28] R. Iordanova, V. Dimitrov, Y. Dimitriev, D. Klissurski, J. Non-Cryst. Solids 180 (1994) 58–65.
[29] S. Vyazovkin, I. Dranca, Macromol. Chem. Phys. 207 (2006) 20–25.